



National Library  
of Canada

Acquisitions and  
Bibliographic Services Branch

395 Wellington Street  
Ottawa, Ontario  
K1A 0N4

Bibliothèque nationale  
du Canada

Direction des acquisitions et  
des services bibliographiques

395, rue Wellington  
Ottawa (Ontario)  
K1A 0N4

*Your file* *Votre référence*

*Our file* *Notre référence*

**The author has granted an irrevocable non-exclusive licence allowing the National Library of Canada to reproduce, loan, distribute or sell copies of his/her thesis by any means and in any form or format, making this thesis available to interested persons.**

**L'auteur a accordé une licence irrévocable et non exclusive permettant à la Bibliothèque nationale du Canada de reproduire, prêter, distribuer ou vendre des copies de sa thèse de quelque manière et sous quelque forme que ce soit pour mettre des exemplaires de cette thèse à la disposition des personnes intéressées.**

**The author retains ownership of the copyright in his/her thesis. Neither the thesis nor substantial extracts from it may be printed or otherwise reproduced without his/her permission.**

**L'auteur conserve la propriété du droit d'auteur qui protège sa thèse. Ni la thèse ni des extraits substantiels de celle-ci ne doivent être imprimés ou autrement reproduits sans son autorisation.**

ISBN 0-612-16490-X

**Canada**

Name Kenneth R. Sills

Dissertation Abstracts International is arranged by broad, general subject categories. Please select the one subject which most nearly describes the content of your dissertation. Enter the corresponding four-digit code in the spaces provided.

Astronomy and Astrophysics

SUBJECT TERM

0606 U.M.I.  
SUBJECT CODE

**Subject Categories**

**THE HUMANITIES AND SOCIAL SCIENCES**

**COMMUNICATIONS AND THE ARTS**

Architecture	0729
Art History	0377
Cinema	0900
Dance	0378
Fine Arts	0357
Information Science	0723
Journalism	0391
Library Science	0399
Mass Communications	0708
Music	0413
Speech Communication	0459
Theater	0465

**EDUCATION**

General	0515
Administration	0514
Adult and Continuing	0516
Agricultural	0517
Art	0273
Bilingual and Multicultural	0282
Business	0688
Community College	0275
Curriculum and Instruction	0727
Early Childhood	0518
Elementary	0524
Finance	0277
Guidance and Counseling	0519
Health	0680
Higher	0745
History of	0520
Home Economics	0278
Industrial	0521
Language and Literature	0279
Mathematics	0280
Music	0522
Philosophy of	0998
Physical	0523

Psychology	0525
Reading	0535
Religious	0527
Sciences	0714
Secondary	0533
Social Sciences	0534
Sociology of	0340
Special	0529
Teacher Training	0530
Technology	0710
Tests and Measurements	0288
Vocational	0747

**LANGUAGE, LITERATURE AND LINGUISTICS**

Language	General	0679
	Ancient	0289
	Linguistics	0290
	Modern	0291
Literature	General	0401
	Classical	0294
	Comparative	0295
	Medieval	0297
	Modern	0298
	African	0316
	American	0591
	Asian	0305
	Canadian (English)	0352
	Canadian (French)	0355
	English	0593
	Germanic	0311
	Latin American	0312
	Middle Eastern	0315
	Romance	0313
	Slavic and East European	0314

**PHILOSOPHY, RELIGION AND THEOLOGY**

Philosophy	0422	
Religion	General	0318
	Biblical Studies	0321
	Clergy	0319
	History of	0320
	Philosophy of	0322
Theology	0469	

**SOCIAL SCIENCES**

American Studies	0323	
Anthropology	Archeology	0324
	Cultural	0326
	Physical	0327
Business Administration	General	0310
	Accounting	0272
	Banking	0770
	Management	0454
	Marketing	0338
Canadian Studies	0385	
Economics	General	0501
	Agricultural	0503
	Commerce-Business	0505
	Finance	0508
	History	0509
	Labor	0510
	Theory	0511
Folklore	0358	
Geography	0366	
Gerontology	0351	
History	General	0578

Ancient	0579	
Medieval	0581	
Modern	0582	
Black	0328	
African	0331	
Asia, Australia and Oceania	0332	
Canadian	0334	
European	0335	
Latin American	0336	
Middle Eastern	0333	
United States	0337	
History of Science	0585	
Law	0398	
Political Science	General	0615
	International Law and Relations	0616
	Public Administration	0617
Recreation	0814	
Social Work	0452	
Sociology	General	0626
	Criminology and Penology	0627
	Demography	0938
	Ethnic and Racial Studies	0631
	Individual and Family Studies	0628
	Industrial and Labor Relations	0629
	Public and Social Welfare	0630
	Social Structure and Development	0700
	Theory and Methods	0344
Transportation	0709	
Urban and Regional Planning	0999	
Women's Studies	0453	

**THE SCIENCES AND ENGINEERING**

**BIOLOGICAL SCIENCES**

Agriculture	General	0473
	Agronomy	0285
	Animal Culture and Nutrition	0475
	Animal Pathology	0476
	Food Science and Technology	0359
	Forestry and Wildlife	0478
	Plant Culture	0479
	Plant Pathology	0480
	Plant Physiology	0817
	Range Management	0777
	Wood Technology	0746
Biology	General	0306
	Anatomy	0287
	Biostatistics	0308
	Botany	0309
	Cell	0379
	Ecology	0329
	Entomology	0353
	Genetics	0369
	Limnology	0793
	Microbiology	0410
	Molecular	0307
	Neuroscience	0317
	Oceanography	0416
	Physiology	0433
	Radiation	0821
	Veterinary Science	0778
	Zoology	0472
Biophysics	General	0786
	Medical	0760

**EARTH SCIENCES**

Biogeochemistry	0425
Geochemistry	0996

Geodesy	0370
Geology	0372
Geophysics	0373
Hydrology	0388
Mineralogy	0411
Paleobotany	0345
Paleoecology	0426
Paleontology	0418
Paleozoology	0985
Palyology	0427
Physical Geography	0368
Physical Oceanography	0415

**HEALTH AND ENVIRONMENTAL SCIENCES**

Environmental Sciences	0768	
Health Sciences	General	0566
	Audiology	0300
	Chemotherapy	095
	Dentistry	0567
	Education	0350
	Hospital Management	0769
	Human Development	0758
	Immunology	0982
	Medicine and Surgery	0544
	Mental Health	0347
	Nursing	0569
	Nutrition	0570
	Obstetrics and Gynecology	0380
	Occupational Health and Therapy	0354
	Ophthalmology	0381
	Pathology	0571
	Pharmacology	0419
	Pharmacy	0572
	Physical Therapy	0382
	Public Health	0573
	Radiology	0574
	Recreation	0575

Speech Pathology	0460
Toxicology	0383
Home Economics	0386

**PHYSICAL SCIENCES**

**Pure Sciences**

Chemistry	General	0485
	Agricultural	0749
	Analytical	0486
	Biochemistry	0487
	Inorganic	0488
	Nuclear	0738
	Organic	0490
	Pharmaceutical	0491
	Physical	0494
	Polymer	0495
	Radiation	0754
Mathematics	0405	
Physics	General	0605
	Acoustics	0986
	Astronomy and Astrophysics	0606
	Atmospheric Science	0608
	Atomic	0748
	Electronics and Electricity	0607
	Elementary Particles and High Energy	0798
	Fluid and Plasma	0759
	Molecular	0609
	Nuclear	0610
	Optics	0752
	Radiation	0756
	Solid State	0611
Statistics	0463	

**Applied Sciences**

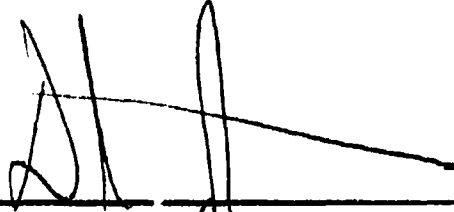
Applied Mechanics	0346
Computer Science	0984

Engineering	General	0537
	Aerospace	0538
	Agricultural	0539
	Automotive	0540
	Biomedical	0541
	Chemical	0542
	Civil	0543
	Electronics and Electrical	0544
	Heat and Thermodynamics	0348
	Hydraulic	0545
	Industrial	0546
	Marine	0547
	Materials Science	0794
	Mechanical	0548
	Metallurgy	0743
	Mining	0551
	Nuclear	0552
	Packaging	0549
	Petroleum	0765
	Sanitary and Municipal	0554
	System Science	0790
Geotechnical	0428	
Operations Research	0796	
Plastics Technology	0795	
Textile Technology	0994	
<b>PSYCHOLOGY</b>	General	0621
	Behavioral	0384
	Clinical	0622
	Developmental	0620
	Experimental	0623
	Industrial	0624
	Personality	0625
	Physiological	0989
	Psychobiology	0349
	Psychometrics	0632
	Social	0451



# Certificate of Examination

Saint Mary's University  
Department of Astronomy and Physics



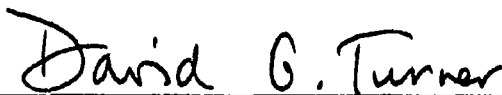
---

Dr. David B. Guenther  
Department of Astronomy and Physics  
Saint Mary's University  
(Thesis Supervisor)



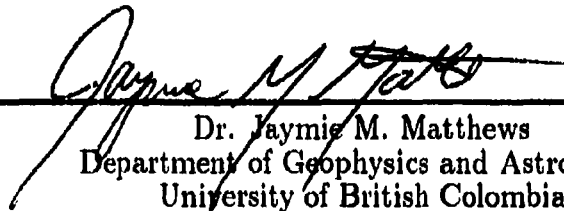
---

Dr. David A. Clarke  
Department of Astronomy and Physics  
Saint Mary's University



---

Dr. David G. Turner  
Department of Astronomy and Physics  
Saint Mary's University



---

Dr. Jaymie M. Matthews  
Department of Geophysics and Astronomy  
University of British Columbia  
(External Reader)

## Abstract

### Seismology of Stars in the Hyades and M67 Open Clusters: Theoretical Constraints on the Mixing Length Parameter

Kenneth Royal Sills

September 1996

The mixing length parameter is a free parameter governing convective energy transport in current stellar models, and is poorly constrained by current photometric observations. Theoretical nonradial pulsation spectra have been calculated for main-sequence stars in the Hyades and M67 open clusters. It is shown that the major eigenfrequency spacing is sensitive to the mixing length parameter, and relatively insensitive to uncertainties in stellar metallicity, age, and helium abundance. Given the predicted uncertainties in observing the major eigenfrequency spacing of stars in the Hyades and M67 clusters, it is shown that proposed seismological studies of these clusters (Gilliland *et al.* 1993; Appourchaux *et al.* 1991) could determine the mixing length parameters for member stars to within  $\pm 0.2$ . The determination of the mixing length parameter for a number of different, well-characterized stars would allow for the parameterization of convective properties as a function of other stellar characteristics. Such a parameterization would be beneficial to current efforts to numerically simulate stellar convection from first principles (Demarque 1996; Kim *et al.* 1996).

# Contents

<i>List of Figures</i>	<i>ii</i>
<i>Acknowledgements</i>	<i>iv</i>
<b>1 Introduction</b>	<b>1</b>
<b>2 Objectives</b>	<b>6</b>
2.1 The Advantages of Stellar Clusters . . . . .	6
2.2 Observational Characteristics . . . . .	7
2.3 Selection of Clusters . . . . .	12
2.4 Determination of the Mixing Length Parameter using a Colour-Magnitude Diagram . . . . .	12
<b>3 Results</b>	<b>17</b>
3.1 The Stellar Models and Pulsation Spectra . . . . .	17
3.2 Uncertainties in the Predictions . . . . .	19
<b>4 Summary and Conclusions</b>	<b>23</b>
<b>Appendix A</b>	<b>26</b>
<b>References</b>	<b>34</b>
<i>Curriculum Vitae</i>	<b>37</b>

# List of Figures

- 1 Diagram showing nodal lines for nonradial oscillations for  $m=0$  and (a)  $\ell=1$ , (b)  $\ell=2$ , and (c)  $\ell=3$ . Red regions represent expansion and blue regions represent contraction. White regions represent nodal lines. Note that the azimuthal degree equals the number of nodal lines. 8
- 2 Colour-colour diagram for models run using Hyades cluster parameters. Each group of 11 points represents the variation of the mixing length parameter from 1.5 to 2.5 in increments of 0.1 for masses from  $0.7 M_{\odot}$  to  $1.5 M_{\odot}$  in increments of  $0.1 M_{\odot}$ . The arrow shows the direction of increasing mixing length parameter. . . . . 14
- 3 Colour-magnitude diagram for models run using Hyades cluster parameters. Each group of 11 points represents the variation of the mixing length parameter from 1.5 to 2.5 in increments of 0.1 for a mass of  $0.7 M_{\odot}$  to  $1.5 M_{\odot}$  in increments of  $0.1 M_{\odot}$ . The arrow shows the direction of increasing mixing length parameter. The shaded envelope represents the region within which the uncertainties in metallicity, helium abundance and age prevent accurate determination of the mixing length parameter. . . . . 15
- 4 Major spacing-absolute visual magnitude diagram for models run using Hyades cluster parameters. Each group of 11 points represents the variation of the mixing length parameter from 1.5 to 2.5 in increments of 0.1 for masses from  $0.7 M_{\odot}$  to  $1.5 M_{\odot}$  in increments of  $0.1 M_{\odot}$ . The arrow shows the direction of increasing mixing length parameter. The shaded envelope represents the region within which the uncertainties in metallicity, helium abundance and age prevent accurate determination of the mixing length parameter. . . . . 20

5 Major spacing-absolute visual magnitude diagram for models run using M67 cluster parameters. Each group of 11 points represents the variation of the mixing length parameter from 1.5 to 2.5 in increments of 0.1 for masses from  $0.7 M_{\odot}$  to  $1.1 M_{\odot}$  in increments of  $0.1 M_{\odot}$ . The arrow shows the direction of increasing mixing length parameter. The shaded envelope represents the region within which the uncertainties in metallicity, helium abundance and age prevent accurate determination of the mixing length parameter. . . . . 21

## **Acknowledgements**

The author would like to thank David Guenther for support, both financial and intellectual. Thanks also go to David Clarke, David Turner and Jaymie Matthews for their work as committee members. Malcolm Butler provided assistance with the bureaucracy above and beyond the call of duty. David Turner provided advice about various aspects of open clusters. Mike West posed insightful questions. Dave Lane provided unrivaled technical support, a necessity for such a project. Mel Blake offered many interesting discussions. Alison Sills helped in all areas.

# 1 Introduction

*“So it seems to me that this development is a beautiful example of those bright occasions when theoreticians enter a new field before all logically necessary data are at hand, proceed on the basis of some clear working hypothesis, and in this manner gain results essential for the later derivation of a more definitive theory.”*

-Martin Schwarzschild, 1961

In 1907, Robert Emden published the first basic text on stellar interiors. In this text Emden proceeded by using the working hypothesis that convection alone was the method by which energy was transported from the centre to the surface of every star. At about the same time, it was shown that radiative transfer can be an efficient energy transport mechanism at the high temperatures found in stars (Schwarzschild 1906). In this work, Karl Schwarzschild developed a criterion which predicts whether a given layer in a star is in convective or radiative equilibrium. Using this criterion, he showed that the atmosphere of the Sun was in radiative equilibrium, contrary to the working hypothesis of Emden (1907). Two decades later, Eddington (1926) wrote the second basic text on stellar interiors. In this text, radiative equilibrium was applied in every star from centre to surface. The question of radiative transfer versus convective transport inspired work by Cowling (1935, 1936) and Biermann (1932, 1935) which fostered the qualitative picture that many stars, our Sun being a prime example, consist of a radiative core surrounded by a convective envelope and a thin radiative atmosphere.

In order to produce more than just a qualitative picture of stellar interiors, it was necessary to model convective energy transport in a quantitative manner. To determine the efficiency of convection as an energy transport mechanism, Biermann (1932) adapted the mixing length theory of convection developed by Ludwig Prandtl (1925). The mixing length theory greatly reduces the complexity of mod-

eling the structure of stars with outer convective regions. It is obviously an oversimplification, but to its credit, its use has produced very accurate predictions of the state of the stellar interior. There now exist many different variations on mixing length theory, but all are based on the principles first developed by Biermann (1932, 1943, 1948), Vitense (1953), and Böhm-Vitense (1958). In this picture, the convective medium is made up of warmer rising and cooler sinking bubbles which travel a distance and then are dissolved into the surrounding medium. The distance that one of these convective elements may travel before dissolution is referred to as the mixing length. This basic picture also assumes that the rising bubbles are identical in size, number, mass, speed and mixing length to the sinking bubbles. Given these assumptions, an expression for convective flux can be formulated in terms of the mixing length (Cox & Guili 1968). Unfortunately, this mixing length cannot be determined by mixing length theory, and is not observable. In the laboratory experiments done by Prandtl (1925), the mixing length scaled as the depth of the convective layer. Taking into account the changes in density that occur in stellar convection zones, changes that did not occur in Prandtl's laboratory fluid, a further assumption that the mixing length is proportional to the local pressure scale height is typically made. This assumption assures that the internal flows of convective elements will have a simple, non-peculiar pattern (Schwarzschild 1961). The constant of proportionality ( $\alpha$ ) is called the mixing length parameter and is a global parameter. Work by Chen & Sofia (1987) using numerical simulations of turbulent, compressible convection has confirmed the assumption that the mixing length is indeed proportional to the local pressure scale height for deep efficient convection. The mixing length parameter,  $\alpha$ , and the helium abundance,  $Y$ , of a star are used as free parameters in stellar modeling. Knowledge of stellar radius and luminosity constrain these parameters as described below.

The efficiency of convective energy transport depends on the mixing length pa-

parameter. A large mixing length parameter implies a large temperature gradient in a convective region. A change in the mixing length parameter has little effect on the luminosity of a star. The spatial extent of a convection zone is determined by the efficiency of that convection zone to transport the energy from its bottom to its top. This is determined by the temperature gradient. Basically, a larger temperature gradient will require a smaller distance to transport a given amount of energy. Thus, a larger mixing length parameter will decrease the stellar radius. For a more complete and physically accurate description see Larson (1974). Since the luminosity is relatively independent of choice of the mixing length parameter, a decrease in stellar radius caused by a larger mixing length parameter will result in an increase in stellar effective temperature. This is observable as a change in the colour of the star.

The mean molecular weight of a star is dependent on the helium mass fraction. Since the majority of a typical star is composed of hydrogen, an increase in the helium mass fraction at the expense of the hydrogen mass fraction will increase the mean molecular weight of a star. Since the luminosity of a star is strongly dependent on its mean molecular weight (see Clayton 1983), a change in the helium abundance affects the luminosity of a star. This is observable as a change in the absolute magnitude of the star.

The ability to constrain these two free parameters is contingent upon the accurate determination of observables such as mass, metallicity, luminosity and temperature. These free parameters are best determined for the Sun. For most field stars, it is necessary to make the assumption that the values of the solar helium abundance and mixing length can be scaled by some simple means to be valid for use in constructing stellar models of a particular field star. This assumption leads to an increased uncertainty in the determination of other relevant parameters such as mass, metallicity and age for that field star. One goal of current research (Demarque 1996;

Kim *et al.* 1996) is to develop a numerical method to model the convective envelope of the Sun and other stars from first principles. Results produced by such an effort will be free from the uncertainties of the mixing length formalism. Thus, it would be very useful to determine the mixing length for a number of different, well-characterized stars. This would allow for the parameterization of convective properties as a function of other stellar parameters and help direct the work on simulating convection from first principles.

The discovery that the surface of the Sun oscillates with a period of about five minutes (Leighton *et al.* 1962) does not obviously fit into a discussion of the mixing length parameter. For some time, the five minute oscillations were thought to be local resonances caused by the overshoot of convective elements into the atmosphere. It was demonstrated by Frazier (1968) that this explanation was inconsistent with spectral analysis of the oscillations. Frazier proposed that the oscillations were primarily a superposition of a large number of standing resonant acoustic waves trapped in subphotospheric layers. Prompted by this, Ulrich (1970) examined the acoustic properties of the subphotospheric layers of the Sun and determined that such acoustic oscillations could only exist along discrete lines in a diagram of horizontal wavenumber versus frequency. This pattern was confirmed observationally by Deubner (1975), but discrepancies between the observations and predictions showed that the contemporary models of the Sun were not correct. This was the birth of the field known as helioseismology. In the last two decades it is a field which has proven to be a window into the inner workings of the Sun. It provides a new set of observables which can be used to constrain the free parameters  $\Upsilon$  and  $\alpha$ .

Knowledge of the solar acoustic spectrum has provided a detailed look at the interior structure of the Sun. Its accurate determination has allowed for the testing of new ideas which push the envelope of modern physics (Demarque *et al.* 1994; Guenther *et al.* 1996). Unfortunately, the intrinsically small amplitudes of these

oscillations make them difficult to observe on stars other than the Sun (Gelly *et al.* 1988). However, the wealth of information that stands to be gained has prompted continual improvement in observational techniques and instrumentation. These efforts have concentrated on two categories of stars: those which are closest to us, and those in clusters. It is to the latter which this thesis is devoted.

## 2 Objectives

### 2.1 The Advantages of Stellar Clusters

Given that only recently has strong evidence for the detection of nonradial, solar-type pulsation been made (Kjeldsen *et al.* 1995), it is logical to ask what advantage there would be to observing stars in open clusters. The open clusters are more distant than many solar-type field stars, and hence pulsation would be less easily detected. However, observing clusters of stars does afford certain advantages.

The primary advantage of observing stellar clusters is that the interpretive value of observed oscillation data increases as knowledge of fundamental stellar parameters improve (Gough 1987; Brown 1991; Guenther & Demarque 1995). Many stellar clusters have been comprehensively studied and the fundamental parameters such as distance, age, and metallicity are known far better for stars in these clusters than for an individual field star. As well, with a stellar ensemble belonging to a cluster, we can assume that all stars have the same distance, age, metallicity and initial helium abundance. For a unique description of a typical star, one requires precise knowledge of six parameters: the stellar mass, age, metallicity, initial helium abundance, distance to the star, and a mixing length parameter (Gilliland & Brown 1992). Thus, differences between stars belonging to a cluster can be studied with four of the six parameters removed. With the addition of oscillation data to the list of independent observables, the opportunity exists to examine the assumptions originally made in defining a typical star.

Secondly, stellar clusters provide a field of view which is populated with *related* stars at a fairly high spatial density. By increasing the number of stars that can be observed in a single exposure, the efficiency of the observations is improved. Given that proposed observations (Gilliland 1995) would require a large time commitment from each of the largest telescopes, efficiency is a necessity.

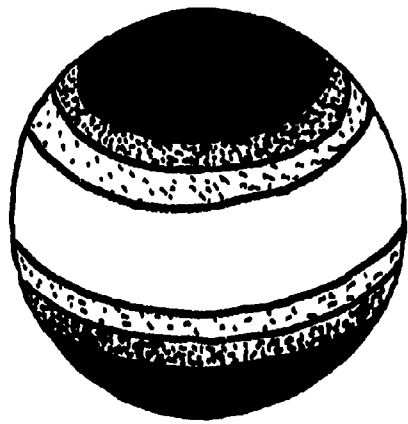
Thus, the increase in difficulty of observing oscillations in stars within clusters, as compared to closer field stars, is compensated for by the increase in the value of the information attained by such observations. Since the observation of stellar pulsation characteristics in cluster stars is such a formidable task, the choice of pulsation characteristic should be limited to that which is realistically obtainable at present.

## 2.2 Observational Characteristics

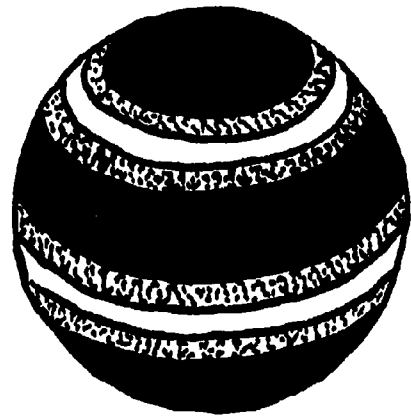
The Sun provides insight into what information can be gleaned from the pulsation spectra of other stars and how difficult it will be to gather that information. Study of the solar Five Minute Oscillation has shown that it is a superposition of about ten million individual resonant waves. Each of these resonant waves, or normal modes of oscillation, can be characterized by three wave numbers:  $n$ ,  $\ell$  and  $m$ . The radial order,  $n$ , roughly gives the number of nodes in the radial direction. The azimuthal degree,  $\ell$ , is related to the horizontal wavenumber,  $k_h$ , at a radius  $r$  by

$$k_h = \frac{\sqrt{\ell(\ell + 1)}}{r}. \quad (1)$$

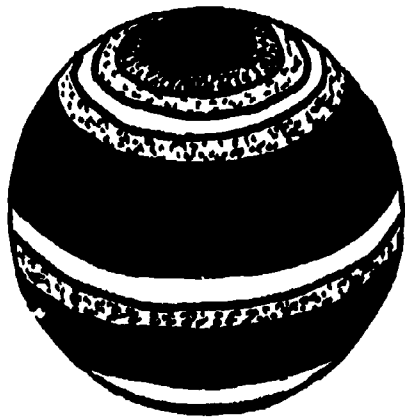
The case  $\ell=0$  describes a mode in which the oscillation expands and contracts spherically in the radial direction. The azimuthal order,  $m$ , is related to the number of nodes around the equator. In principle, the frequency of a mode of oscillation depends on all three wavenumbers. If rotation and other departures from spherical symmetry are ignored, then the frequency is independent of the azimuthal order. Figure 1 depicts cases  $\ell=1, 2$  and  $3$  for  $m=0$  nonradial oscillations. In this thesis, consideration will be limited to stars for which departures from spherical symmetry are typically small. Thus, this work will assume that the frequency is independent of azimuthal order.



(a)  $l=1$



(b)  $l=2$



(c)  $l=3$

Figure 1: Diagram showing nodal lines for nonradial oscillations for  $m=0$  and (a)  $l=1$ , (b)  $l=2$ , and (c)  $l=3$ . Red regions represent expansion and blue regions represent contraction. White regions represent nodal lines. Note that the azimuthal degree equals the number of nodal lines.

The Five Minute Oscillation is comprised of resonant waves for which the restoring force is pressure. These are referred to as p-mode oscillations. Each p-mode is a trapped sound wave; thus, each p-mode carries information about the average sound speed over its path of travel. Since higher degree p-modes are increasingly confined to a region close to the surface, by observing  $\ell=0$  modes one can determine the global average sound speed. By then observing  $\ell=1$  modes one can determine the average sound speed in a region encompassing all but the most central region. With these two averages one can determine the sound speed local to the region where the  $\ell=1$  mode is evanescent. One can resolve the run of sound speed with radius by continuing this process to higher and higher degree provided that it is possible to spatially resolve the modes with high azimuthal degree. The Sun is the one star for which it is currently possible to spatially resolve modes with azimuthal degree higher than about three or four. Observations of stars other than the Sun are limited by the lack of this spatial resolution. On an unresolved stellar surface, oscillations which have many nodes simultaneously visible are averaged out, and thus yield no information. Thus, this work will focus on modes with degrees  $\ell=0,1,2,3$ . This limits the determination of the structure of stars other than the Sun to more global properties.

Vandakurov (1967) showed that modes of low-degree (*i.e.*  $\ell \ll n$ ) should satisfy a dispersion relation of the form

$$\nu_{n,\ell} = \left(n + \frac{1}{2}(\ell + \frac{1}{2}) + \alpha\right)\nu_0 + \epsilon_{n,\ell}, \quad (2)$$

where  $\nu_{n,\ell}$  is the frequency of the mode with radial order  $n$  and azimuthal degree  $\ell$ ,  $\alpha$  is related to the polytropic index of the outer layers of the stellar envelope and is of the order 1,  $\epsilon_{n,\ell}$  is a second order correction term (Tassoul 1980), and  $\nu_0$  is the characteristic asymptotic frequency spacing, defined here as

$$\nu_0 = \left[ 2 \int_0^R \frac{dr}{c_s} \right]^{-1} \quad (3)$$

where  $R$  is the radius of the star and  $c_s$  is the sound speed at distance  $r$  from the centre. The characteristic asymptotic frequency spacing is thus a global constant for a given star. One can show that to first order, the dispersion relation presented by Vandakurov (1967) reduces to

$$\nu_{n,\ell} \sim \left[ n + \frac{1}{2}\ell \right] \nu_0 + C, \quad (4)$$

where  $C$  is independent of both degree and radial order, and is small for  $\ell \ll n$ . Thus, a set of equally spaced frequencies are found for a given  $\ell \ll n$ , and the spacing between each frequency,

$$\nu_{n,\ell} - \nu_{n-1,\ell} \sim \nu_0 \quad (5)$$

is  $\nu_0$ , the characteristic asymptotic frequency spacing. In this work, the characteristic asymptotic frequency spacing is approximated using

$$\bar{\nu}_0 = \frac{\sum_{n=15}^{30} [\nu_{n,\ell} - \nu_{n-1,\ell}]}{16} \sim \nu_0, \quad (6)$$

where  $\bar{\nu}_0$  is called the major spacing.

Using equation 4 for different degrees one can show that

$$\nu_{n,\ell} - \nu_{n,\ell-1} \sim \frac{\nu_0}{2}. \quad (7)$$

Thus, a star will exhibit a power spectrum which resembles a picket fence, and the spacing between pickets will be  $\frac{\nu_0}{2}$ . Promising evidence for such a distribution of oscillation frequencies has been observed recently (Kjeldsen *et al.* 1995) on the

star  $\eta$  Bootes. The first parameter determined from the frequency spectrum of  $\eta$  Bootes was the major spacing. Essentially, a correlation function was used to distinguish the presence of the regularly spaced peaks in the power spectrum caused by a genuine p-mode signal from the observational noise. A well-defined hump in the correlation function indicates the presence of a regular spacing, and this hump occurs at a spacing equal to half of the major spacing. In practice, when looking at real data, the picket fence described above has noise added to it. The correlation function tries to match an equally-spaced picket fence to the noisy observed power spectrum, and counts the number of peaks that match up for each different spacing of picket fence. The distribution with the spacing that matches the largest number of peaks in the observed power spectrum has a spacing equal to half the major spacing,  $\frac{\nu_0}{2}$ . Once this spacing is determined, peaks in the power spectrum resulting from actual oscillations are more easily identified. In this way, the major spacing is the most immediately available, and least uncertain, observable parameter to be acquired from a stellar oscillation spectra.

The major spacing is related to stellar mass and radius by

$$\bar{\nu}_0 \propto \left(\frac{M}{R^3}\right)^{\frac{1}{2}}. \quad (8)$$

That is, the major spacing is directly proportional to the mean density of the star. The major spacing of a star is therefore a useful, and realistically observable, parameter which is not currently being exploited for solar-type oscillators. Furthermore, the strong dependence of the major spacing on the stellar radius suggests that it may function as a probe of the mixing length parameter, since the stellar radius is a strong function of the choice of mixing length. It will be shown in this work that the major spacing is much less sensitive to realistic changes in helium abundance, age and metallicity than it is to realistic changes in the mixing length

parameter. Thus, the major spacing is a parameter which can be used to decouple the uncertainty in the mixing length parameter from the uncertainties in other stellar parameters.

### **2.3 Selection of Clusters**

To best constrain the mixing length parameter, open cluster selection should be limited to clusters for which observable parameters are accurately known. Two such clusters are the targets of proposed observational campaigns: M67 (Gilliland *et al.* 1995) and the Hyades (Appourchaux *et al.* 1991). This thesis is focussed on these two clusters. Values used in this thesis for cluster age, metallicity and helium abundance are given below.

For M67, the cluster age was taken to be  $4.0 \pm 0.5$  Gyr (Dinescu *et al.* 1995), and the cluster metallicity was taken to be  $Z=0.017 \pm 0.004$  (Chaboyer *et al.*, 1995). The helium abundance and its uncertainty were calculated using the above metallicity value and its uncertainty in the enrichment equation  $(Y - Y_{\odot}) = 2.5(Z - Z_{\odot})$  (Chaboyer *et al.* 1995).

For the Hyades, the cluster age was taken to be 0.67 Gyr (Boesgaard 1989) with an uncertainty of  $\pm 0.05$  Gyr. The cluster metallicity was taken to be  $Z=0.024$  (Taylor 1994) with an uncertainty of  $\pm 0.004$ . The helium abundance and its uncertainty were calculated using the above metallicity value and its uncertainty in same manner as for M67.

### **2.4 Determination of the Mixing Length Parameter using a Colour-Magnitude Diagram**

To demonstrate that neither colour-magnitude diagram analysis, nor colour-colour diagram analysis can sufficiently constrain the mixing length parameter given ob-

servational uncertainties, both a theoretical colour-magnitude diagram and *UBV* colour-colour diagram were generated for the Hyades. For the “best” values as given in the previous section, stellar models were constructed for masses from  $0.7 M_{\odot}$  to  $1.5 M_{\odot}$  in  $0.1 M_{\odot}$  increments. For each of the masses, models having mixing length parameters from 1.5 to 2.5 in increments of 0.1 were generated. Evolutionary tracks were constructed using the Yale Rotating Evolution Code (YREC) (Guenther, Jaffe & Demarque 1989) in its nonrotating configuration using the OPAL opacities, Kurucz (1991) opacities for temperatures below  $\log T = 4.0$ , and the Anders & Grevesse (1989) solar mixture of metals. Colours and absolute magnitudes were calculated using the method described in Green *et al.* (1987). Appendix A shows model characteristics for all stellar models constructed using Hyades cluster parameters.

Figure 2 shows the *UBV* colour-colour diagram of the constructed models. The spread caused by varying the mixing length parameter is parallel to the direction of increasing stellar mass; hence, isochrone fitting will yield no extra information about the mixing length parameter. The *UBV* colour-colour diagram was chosen to demonstrate this, but all colour-colour diagrams in the *UBVRI* system were found to suffer similarly from this problem.

Figure 3 shows the colour-magnitude diagram of the constructed models. The spread caused by varying the mixing length parameter is not completely parallel to the direction of increasing stellar mass. Discrimination of the mixing length parameter to uncertainty levels of  $\pm 0.1$  would be possible with *U-B* colour determinations accurate to 0.02 magnitude if no uncertainty existed in other modeling parameters.

To investigate the effects of the known uncertainties in the modeling parameters, additional stellar models were constructed. The masses of these models ranged from  $0.7 M_{\odot}$  to  $1.5 M_{\odot}$  in  $0.1 M_{\odot}$  increments. Each model was evolved with a mixing length parameter of 2.0. For each mass, four extreme models were evolved and their pulsation spectra were calculated. One model was evolved with both the cluster age

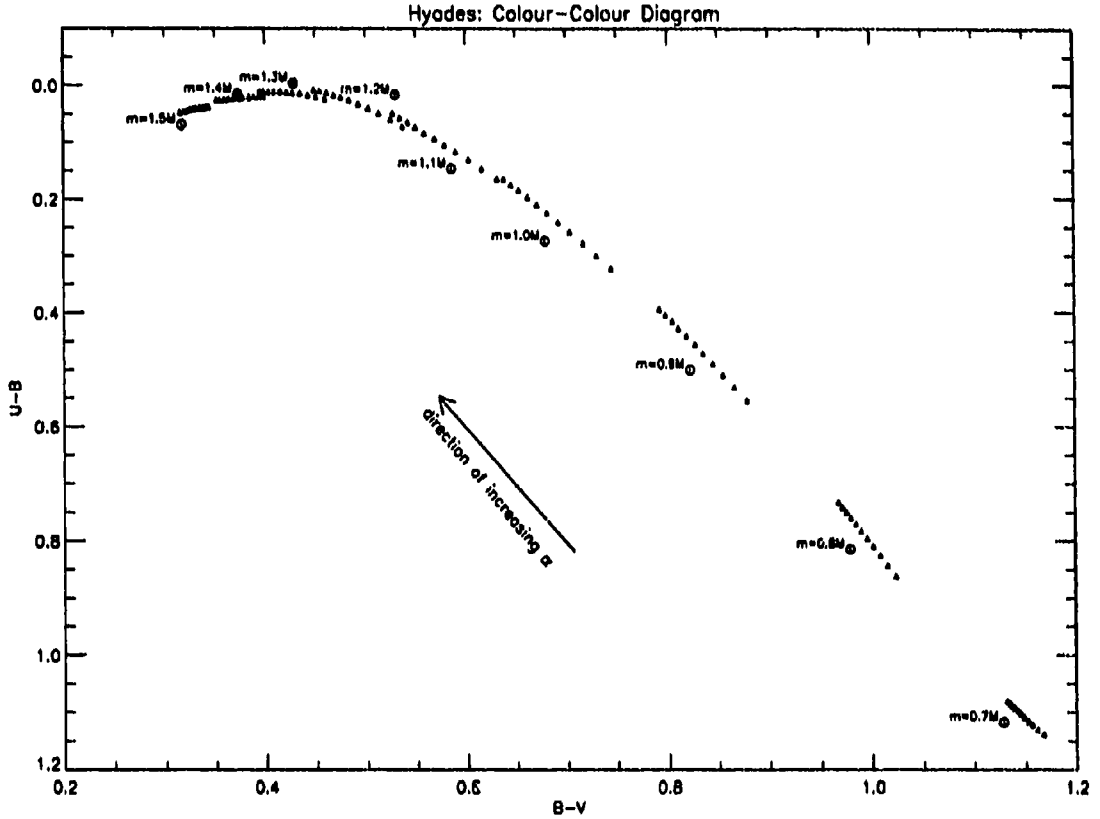


Figure 2: Colour-colour diagram for models run using Hyades cluster parameters. Each group of 11 points represents the variation of the mixing length parameter from 1.5 to 2.5 in increments of 0.1 for masses from  $0.7 M_{\odot}$  to  $1.5 M_{\odot}$  in increments of  $0.1 M_{\odot}$ . The arrow shows the direction of increasing mixing length parameter.

and metallicity at the maximum value allowed by observational uncertainties. One model was evolved with both the cluster age and metallicity at the minimum value allowed by observational uncertainties. One model was evolved with the cluster age at a minimum and the metallicity at a maximum. One model was evolved with the cluster age at a maximum and the metallicity at a minimum. It was assumed that low values of metallicity only occur in conjunction with low values of helium abundance, and conversely that high values of metallicity only occur in conjunction with high values of helium abundance. This assumption is consistent with the current understanding of galactic chemical enrichment. The uncertainties in the metallicity, age and helium abundance define an area of uncertainty shown

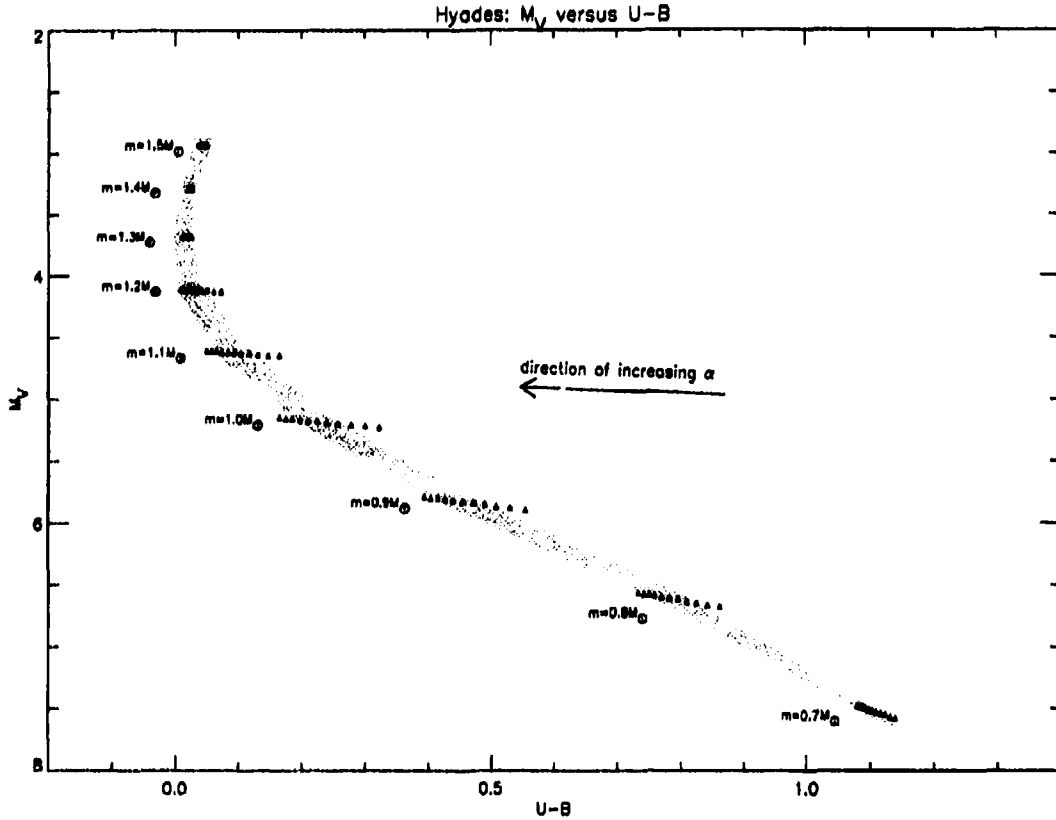


Figure 3: Colour-magnitude diagram for models run using Hyades cluster parameters. Each group of 11 points represents the variation of the mixing length parameter from 1.5 to 2.5 in increments of 0.1 for a mass of  $0.7 M_{\odot}$  to  $1.5 M_{\odot}$  in increments of  $0.1 M_{\odot}$ . The arrow shows the direction of increasing mixing length parameter. The shaded envelope represents the region within which the uncertainties in metallicity, helium abundance and age prevent accurate determination of the mixing length parameter.

as a shaded region in Figure 3. Taking this area of uncertainty to represent the outermost error boundary implicitly assumes a linear response to the perturbations in metallicity, helium abundance and age. This assumption is justified because the perturbations are relatively small, so to first order the response of the system will be directly proportional to the relative size of the perturbation. It is apparent from this figure that a colour-magnitude diagram cannot sufficiently decouple the uncertainty in the mixing length parameter from the uncertainties in other cluster parameters. At best, this method could constrain the mixing length parameter to  $\pm 0.3$  for stars of masses between  $0.9 M_{\odot}$  and  $1.0 M_{\odot}$ . This precision rapidly degrades for stars of

masses higher than  $1.1 M_{\odot}$  and lower than  $0.9 M_{\odot}$ . Such a level of precision is not sufficient to probe changes in the mixing length parameter with mass, and may not be sufficient to determine whether the mixing length parameter is constant for stars of the same mass.

## 3 Results

### 3.1 The Stellar Models and Pulsation Spectra

The purpose of this study is to determine whether the observation of pulsation spectra of main-sequence stars in nearby open clusters would provide a constraint on the mixing length parameter. To do this, evolutionary tracks were constructed using YREC in the configuration described in section 2.4. Stellar models were evolved for both the Hyades and M67 open clusters.

For the Hyades, evolutionary tracks were constructed for stars of masses from  $0.7 M_{\odot}$  to  $1.5 M_{\odot}$  using an increment of one-tenth of a solar mass. For each of these masses, tracks were evolved with the mixing length parameter being varied from 1.5 to 2.5 in increments of 0.1. Hence, 99 models were produced in mass-mixing length space. Individual models were evolved to a current best estimate for cluster age (Boesgaard 1989) and metallicity (Taylor 1994). The helium abundance for the Hyades was chosen assuming the helium enrichment parameter  $R=2.5$  (Chaboyer, Demarque & Pinsonneault 1995), where  $R=(\Delta Y/\Delta Z)$ .

For M67, evolutionary tracks were constructed for stars of masses from 0.7 to 1.1 times solar using an increment of one-tenth of a solar mass. For each of these masses, tracks were evolved with the mixing length parameter being varied from 1.5 to 2.5 in increments of 0.1. Hence, 55 models were produced in mass-mixing length space. Individual models were evolved to a current best estimate for the cluster age (Dinescu, Demarque, Guenther, & Pinsonneault, 1995) and metallicity (Chaboyer *et al.* 1995). The helium abundance and its uncertainty were calculated using the above metallicity value and its uncertainty in same manner as for M67.

The pulsation spectrum for each evolved model was calculated by using Guenther's nonradial, nonadiabatic stellar pulsation code in its adiabatic configuration (Guenther 1994). Presently, nonadiabatic effects are negligible when compared with

observational error and, thus, have been left out in favour of increased speed of calculation. The pulsation code calculated frequencies of modes with radial orders  $n=15$  to 30 and azimuthal orders  $\ell=0$  to 3, and these frequencies were used to calculate the major spacing for each evolved model.

Absolute visual magnitudes were calculated using the method described in Green *et al.* (1987). This method is currently used to produce the Yale '95 Isochrones (Demarque 1996).

Figures 4 and 5 show the plot of major spacing versus absolute visual magnitude for stellar models evolved with Hyades cluster parameters and M67 cluster parameters, respectively. These plots demonstrate the dependence of the major spacing on both mass and mixing length.

The major spacing is most sensitive to changes in the mixing length parameter at masses near solar, with sensitivity tapering off at both higher and lower masses. This two-sided taper is produced by the competition of two effects. The first can be explained by looking at the definition of the mixing length parameter. A more massive, more centrally condensed star has a larger value for its pressure scale height than a less massive, less centrally condensed star. Since the mixing length parameter is a measure of the number of pressure scale-heights a convective element moves before it dissolves into its surroundings, a change in the mixing length parameter has a more pronounced effect on the spatial extent of a convection zone in a more massive star. Since a change in the mixing length parameter has little effect on the star below the outer convection zone, the change in radius of the convection zone will change the overall radius of the star. This change in overall radius will affect the major spacing as shown by equation 8. Thus, the spread in major spacing caused by varying the mixing length parameter should increase with mass.

The second effect acts in the opposing direction. It has been well-established by stellar modeling that very-low mass stars are completely convective. Stars with

masses greater than about  $0.4 M_{\odot}$  develop a radiative core. With increasing mass, this radiative core becomes a larger fraction of a star and the outer convective zone become smaller in spatial extent. In Figures 4 and 5, the spread in major spacing caused by varying the mixing length parameter begins to decrease with mass for masses greater than about  $1.1 \odot$ . At this point, though the effect that the mixing length parameter has on the spatial extent of the convective zone is still increasing with mass, the size of the convection zone has become so small as to make the change in overall radius small. Thus, the spread in major spacing caused by varying the mixing length parameter begins to decrease with mass beyond about  $1.1 \odot$ , and the cigar-like shape is produced.

### 3.2 Uncertainties in the Predictions

The effect of uncertainties in helium abundance, metallicity and age was explored by evolving and pulsing models with all realistic combinations of these input parameters. For each mass, four extreme models were evolved and pulsed. One model was evolved with both the cluster age, and metallicity (and hence the helium abundance) at the maximum value allowed by observational uncertainties. One model was evolved with both the cluster age, and metallicity at the minimum value allowed by observational uncertainties. One model was evolved with the cluster age at a minimum and the metallicity at a maximum. One model was evolved with the cluster age at a maximum and the metallicity at a minimum. All of these models were evolved using a mixing length parameter of  $\alpha = 2.0$ . These extreme models were run for both M67 and the Hyades clusters.

By placing the above models of either cluster on a major spacing-absolute visual magnitude diagram and connecting points of equal metallicity and age, but different mass, an envelope is created which defines the region of uncertainty for that cluster.

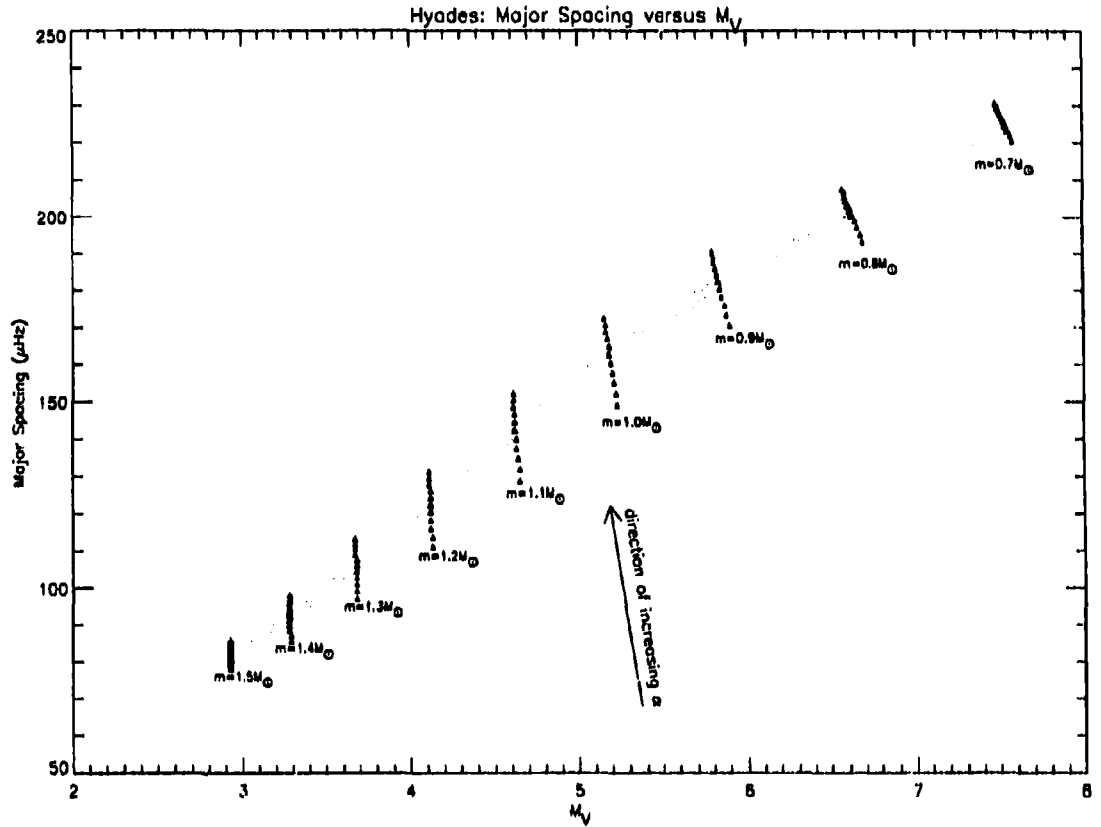


Figure 4: Major spacing-absolute visual magnitude diagram for models run using Hyades cluster parameters. Each group of 11 points represents the variation of the mixing length parameter from 1.5 to 2.5 in increments of 0.1 for masses from  $0.7 M_\odot$  to  $1.5 M_\odot$  in increments of  $0.1 M_\odot$ . The arrow shows the direction of increasing mixing length parameter. The shaded envelope represents the region within which the uncertainties in metallicity, helium abundance and age prevent accurate determination of the mixing length parameter.

This region of uncertainty is represented by the shaded regions on Figures 4 and 5. Appendix A tabulates model characteristics for all stellar models constructed.

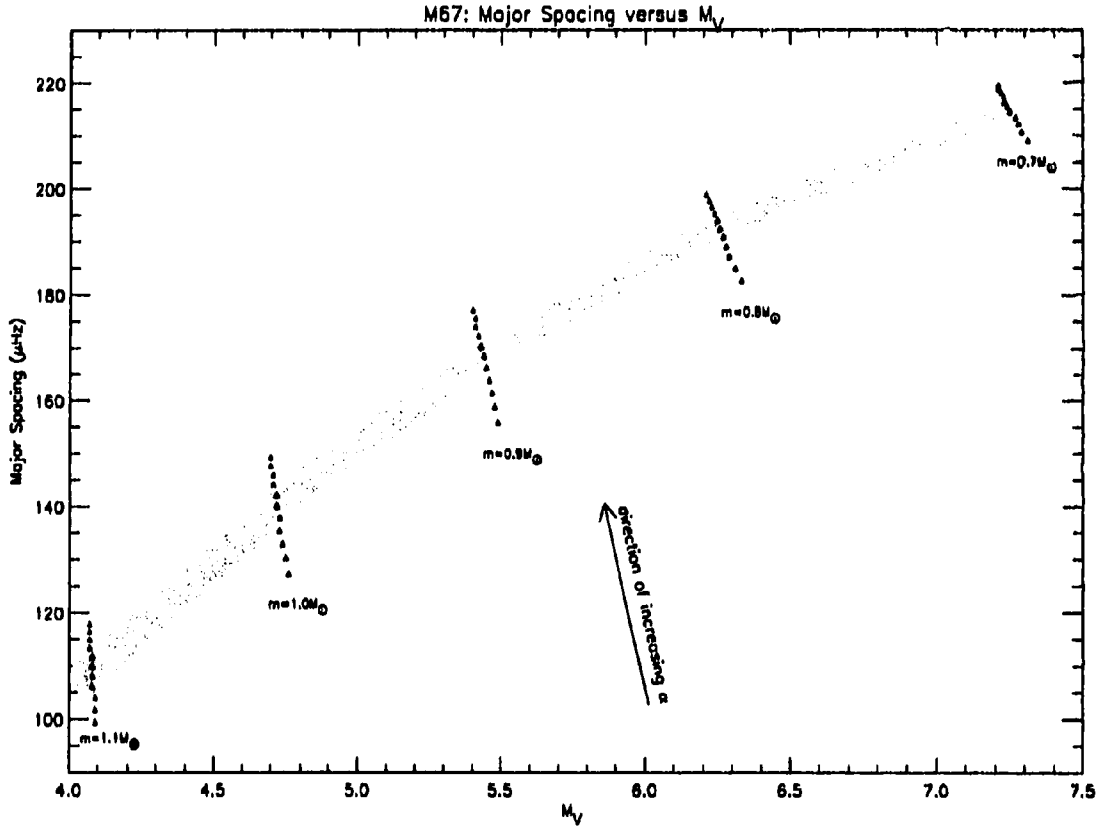


Figure 5: Major spacing-absolute visual magnitude diagram for models run using M67 cluster parameters. Each group of 11 points represents the variation of the mixing length parameter from 1.5 to 2.5 in increments of 0.1 for masses from  $0.7 M_\odot$  to  $1.1 M_\odot$  in increments of  $0.1 M_\odot$ . The arrow shows the direction of increasing mixing length parameter. The shaded envelope represents the region within which the uncertainties in metallicity, helium abundance and age prevent accurate determination of the mixing length parameter.

Uncertainties in the determination of absolute magnitudes for M67 and Hyades cluster stars will limit the ability of seismological observations to accurately constrain the mixing length parameter. The ability to distinguish trends in the mixing length parameter within a cluster is dependent upon the internal accuracy of the absolute magnitude determinations. As well, the ability to compare the mixing length parameters measured for stars in one cluster to the Sun or other clusters is dependent on the external accuracy of the absolute magnitude determinations. For

the Hyades cluster, internal uncertainties are small enough that they do not significantly impact the determination of trends in the mixing length parameter. Recent investigations of the Hyades constrain the external error to less than  $\pm 0.07$  mag (Peterson *et al.* 1993; Dombrowski *et al.* 1991; Gatewood *et al.* 1992). For M67, internal uncertainties are also small. Most recent investigations of M67 constrain the external error to less than  $\pm 0.10$  mag (Nissen *et al.* 1987; Vandenberg & Poll 1989; Demarque *et al.* 1992; Montgomery *et al.* 1993; Tripicco *et al.* 1993). Results from the Hipparcos satellite mission should greatly reduce the uncertainty for the Hyades. Uncertainty in the absolute magnitudes of M67 cluster members will constrain the ability of the technique to determine the mixing length parameter, but will not significantly affect the ability to distinguish trends in the mixing length parameter within the cluster.

## 4 Summary and Conclusions

In proposing a Next Generation Network, Gilliland *et al.* (1995) suggested that such a campaign necessarily required an effort on the part of theorists to justify such a time commitment of the largest telescopes. One such justification has been shown here. Seismological data from stars in stellar clusters could be used to parameterize convection as a function of other stellar properties. Such a parameterization could test whether numerical simulations of convection currently being developed for the Sun can adequately model the convection occurring on other stars. A detailed understanding of the physics underlying stellar convection will eliminate the need for the mixing length formalism. This will allow for more accurate and reliable prediction of stellar parameters such as age and luminosity.

The previous attempt by Gilliland *et al.* (1995) to observe stellar pulsation in cluster members has produced promising results, but no strong evidence that detailed pulsation spectra can be obtained for such stars using current techniques. For that reason, this work has concentrated on determining whether or not the major spacing alone can provide new, useful information about stellar structure. The major spacing will be the most easily determined information to come out of the observation of stellar pulsation. Also, since the major spacing is an average property of the oscillations, its determination will improve as the oscillation frequencies become better determined.

The work done here has shown that the mixing length parameters for stars in the Hyades and M67 clusters can be determined by using the major spacing as a constraint. If the pulsation spectra of stars in these clusters could be measured with the same accuracy as the solar pulsation spectra, mixing length parameters could be determined to within  $\pm 0.1$ . This limit is imposed by the uncertainties in metallicities, helium abundances, and ages of these stars. By using simulated pulsa-

tion spectra, Gilliland *et al.* (1995) estimated the uncertainty in the measurement of the major spacing of stars in M67 at about  $\pm 2\mu\text{Hz}$ . With such an uncertainty, mixing length parameters could be determined to within  $\pm 0.2$ . The recent observations of  $\eta$  Boo by Kjeldsen *et al.* (1995) support the claims that the major spacing can be measured for stars other than our Sun. Observations done by Kjeldsen *et al.* (1995) show that the major spacing for  $\eta$  Boo is determined to an accuracy of about  $\pm 1\mu\text{Hz}$ . The ability to measure the mixing length parameter of these stars will increase as observations improve. Given the uncertainties currently expected in such observations, determination of mixing length using the major spacing is a realistic possibility. It has also been shown here that such a determination cannot be made realistically using CMD fitting.

The question must be asked whether the mixing length should be expected to vary from star to star. It is possible that the characteristics of convection in the Sun can be transferred from star to star by scaling to the pressure scale height. Chaboyer *et al.* (1995) constructed isochrones for 40 globular clusters and fit them to their corresponding observations. In that work it is shown that a solar mixing length parameter,  $\alpha = 1.7$ , yields a good fit for all examined clusters. The evidence for this is the good agreement between theoretical and observed post-main-sequence stars, primarily on the giant branch. However, this work does not consider the possibility that the mixing length parameter may vary from star to star. The mixing length parameter that they derive is a best median value for the cluster as a whole. Their work shows directly that many individual stars do exist that could be better modeled by using non-solar mixing length parameters than by using the solar mixing length parameter.

Other evidence for a mixing length which does not scale to solar as expected has been shown by detailed evolutionary models of  $\alpha$  Cen A and B (Edmonds *et al.* 1992). It was shown that  $\alpha$  Cen A requires a smaller mixing length parameter

than does its companion  $\alpha$  Cen B. Given that both stars in this system should have the same age, metallicity and initial helium abundance, such a distinction could be taken as an indication that the mixing length parameter may vary with mass.

There exist many important factors which are not incorporated into stellar modeling. Uncertainty in the treatment of convection may mask the effects of magnetic fields, diffusion, gravitational settling, convective overshoot and rotation. It is unlikely that with such a simplistic formalism for the treatment of convection one could produce stellar models which are accurate enough to probe such effects. The construction of a model for convection based on fundamental physics can help to clear the way for such detailed analyses. A parameterization of the mixing length parameter using cluster members will provide the large data set needed to establish a detailed, universal model of stellar convection.

The results of this work alone are not reason enough to justify the large observational commitment necessary to determine the pulsation spectra of cluster members in M67 or in the Hyades. This work does provide evidence that successful observations will produce unique constraints on stellar structure. Effort is needed on the part of the theoretical community to provide other such justifications. By providing a large database of stars with well-known structure, the observation of solar-type pulsation on stars in clusters will help to define what problems are present in the current theories of stellar structure and evolution.

# Appendix A

Table 1: Model characteristics for stars evolved using Hyades parameters.

Mass [ $M_{\odot}$ ]	Z	Y	age [Gyr]	$\alpha$	U-B [mag]	B-V [mag]	V-R [mag]	R-I [mag]	$M_v$ [mag]	$i_0$ [ $\mu$ Hz]
0.7	0.028	31	0.62	2.0	1.139	1.162	0.700	0.590	7.54	222.73
0.7	0.028	31	0.72	2.0	1.139	1.162	0.700	0.589	7.53	222.46
0.7	0.024	29	0.67	1.5	1.139	1.167	0.708	0.600	7.58	220.46
0.7	0.024	29	0.67	1.6	1.131	1.161	0.703	0.595	7.57	221.96
0.7	0.024	29	0.67	1.7	1.123	1.156	0.699	0.591	7.55	223.28
0.7	0.024	29	0.67	1.8	1.116	1.152	0.695	0.587	7.54	224.53
0.7	0.024	29	0.67	1.9	1.109	1.148	0.692	0.584	7.53	225.65
0.7	0.024	29	0.67	2.0	1.103	1.145	0.689	0.581	7.52	226.61
0.7	0.024	29	0.67	2.1	1.098	1.142	0.686	0.578	7.51	227.56
0.7	0.024	29	0.67	2.2	1.093	1.139	0.683	0.576	7.50	228.38
0.7	0.024	29	0.67	2.3	1.089	1.136	0.681	0.574	7.49	229.16
0.7	0.024	29	0.67	2.4	1.085	1.134	0.679	0.572	7.49	229.86
0.7	0.024	29	0.67	2.5	1.081	1.131	0.677	0.570	7.48	230.50
0.7	0.020	27	0.62	2.0	1.106	1.152	0.699	0.594	7.60	227.14
0.7	0.020	27	0.72	2.0	1.106	1.152	0.699	0.594	7.60	226.85
0.8	0.028	31	0.62	2.0	0.809	1.000	0.567	0.480	6.60	199.03
0.8	0.028	31	0.72	2.0	0.807	0.999	0.567	0.479	6.60	198.77
0.8	0.024	29	0.67	1.5	0.862	1.023	0.589	0.499	6.68	193.17
0.8	0.024	29	0.67	1.6	0.843	1.015	0.582	0.493	6.67	195.20
0.8	0.024	29	0.67	1.7	0.826	1.008	0.576	0.489	6.65	197.13
0.8	0.024	29	0.67	1.8	0.810	1.001	0.571	0.485	6.64	198.88
0.8	0.024	29	0.67	1.9	0.796	0.995	0.566	0.481	6.62	200.47
0.8	0.024	29	0.67	2.0	0.783	0.989	0.562	0.478	6.61	201.83
0.8	0.024	29	0.67	2.1	0.771	0.984	0.558	0.475	6.60	203.15
0.8	0.024	29	0.67	2.2	0.760	0.979	0.554	0.472	6.59	204.39
0.8	0.024	29	0.67	2.3	0.751	0.975	0.551	0.470	6.58	205.54
0.8	0.024	29	0.67	2.4	0.742	0.971	0.548	0.467	6.58	206.58
0.8	0.024	29	0.67	2.5	0.733	0.967	0.545	0.465	6.57	207.48
0.8	0.020	27	0.62	2.0	0.777	0.987	0.564	0.482	6.66	203.80
0.8	0.020	27	0.72	2.0	0.775	0.987	0.563	0.482	6.66	203.52

Mass [ $M_{\odot}$ ]	Z	Y	age [Gyr]	$\alpha$	U-B [mag]	B-V [mag]	V-R [mag]	R-I [mag]	$M_v$ [mag]	$\bar{\nu}_0$ [ $\mu\text{Hz}$ ]
0.9	0.028	31	0.62	2.0	0.478	0.833	0.457	0.401	5.81	179.46
0.9	0.028	31	0.72	2.0	0.476	0.832	0.456	0.401	5.80	179.10
0.9	0.024	29	0.67	1.5	0.555	0.877	0.485	0.424	5.90	170.60
0.9	0.024	29	0.67	1.6	0.531	0.865	0.478	0.419	5.88	173.39
0.9	0.024	29	0.67	1.7	0.509	0.854	0.471	0.414	5.87	175.93
0.9	0.024	29	0.67	1.8	0.490	0.844	0.464	0.409	5.85	178.27
0.9	0.024	29	0.67	1.9	0.472	0.834	0.459	0.405	5.84	180.42
0.9	0.024	29	0.67	2.0	0.456	0.826	0.454	0.402	5.83	182.41
0.9	0.024	29	0.67	2.1	0.441	0.818	0.449	0.398	5.82	184.25
0.9	0.024	29	0.67	2.2	0.428	0.810	0.444	0.395	5.81	185.95
0.9	0.024	29	0.67	2.3	0.416	0.804	0.441	0.392	5.80	187.52
0.9	0.024	29	0.67	2.4	0.404	0.797	0.437	0.390	5.80	189.00
0.9	0.024	29	0.67	2.5	0.394	0.791	0.434	0.387	5.79	190.38
0.9	0.020	27	0.62	2.0	0.435	0.819	0.452	0.403	5.87	185.61
0.9	0.020	27	0.72	2.0	0.433	0.818	0.451	0.403	5.86	185.27
1.0	0.028	31	0.62	2.0	0.247	0.688	0.379	0.346	5.16	159.33
1.0	0.028	31	0.72	2.0	0.245	0.687	0.378	0.345	5.15	158.81
1.0	0.024	29	0.67	1.5	0.323	0.744	0.407	0.370	5.23	149.05
1.0	0.024	29	0.67	1.6	0.300	0.729	0.400	0.364	5.22	152.20
1.0	0.024	29	0.67	1.7	0.278	0.716	0.393	0.359	5.21	155.11
1.0	0.024	29	0.67	1.8	0.258	0.703	0.387	0.354	5.20	157.81
1.0	0.024	29	0.67	1.9	0.241	0.692	0.381	0.350	5.19	160.33
1.0	0.024	29	0.67	2.0	0.225	0.681	0.376	0.345	5.18	162.66
1.0	0.024	29	0.67	2.1	0.210	0.671	0.371	0.342	5.18	164.84
1.0	0.024	29	0.67	2.2	0.197	0.662	0.367	0.338	5.17	166.88
1.0	0.024	29	0.67	2.3	0.185	0.653	0.363	0.335	5.16	168.79
1.0	0.024	29	0.67	2.4	0.175	0.645	0.359	0.332	5.16	170.58
1.0	0.024	29	0.67	2.5	0.165	0.638	0.356	0.329	5.15	172.26
1.0	0.020	27	0.62	2.0	0.201	0.674	0.373	0.346	5.22	166.58
1.0	0.020	27	0.72	2.0	0.199	0.673	0.372	0.346	5.21	166.10

Mass [ $M_{\odot}$ ]	Z	Y	age [Gyr]	$\alpha$	U-B [mag]	B-V [mag]	V-R [mag]	R-I [mag]	$M_v$ [mag]	$\nu_0$ [ $\mu\text{Hz}$ ]
1.1	0.028	31	0.62	2.0	0.114	0.575	0.324	0.304	4.59	138.94
1.1	0.028	31	0.72	2.0	0.113	0.574	0.324	0.303	4.58	138.22
1.1	0.024	29	0.67	1.5	0.165	0.631	0.351	0.328	4.65	128.80
1.1	0.024	29	0.67	1.6	0.147	0.616	0.344	0.322	4.65	131.85
1.1	0.024	29	0.67	1.7	0.131	0.603	0.338	0.317	4.64	134.71
1.1	0.024	29	0.67	1.8	0.117	0.590	0.332	0.312	4.63	137.39
1.1	0.024	29	0.67	1.9	0.105	0.579	0.326	0.307	4.63	139.91
1.1	0.024	29	0.67	2.0	0.094	0.569	0.322	0.303	4.62	142.27
1.1	0.024	29	0.67	2.1	0.084	0.559	0.317	0.299	4.62	144.49
1.1	0.024	29	0.67	2.2	0.074	0.550	0.313	0.296	4.62	146.58
1.1	0.024	29	0.67	2.3	0.065	0.542	0.309	0.292	4.61	148.55
1.1	0.024	29	0.67	2.4	0.057	0.534	0.305	0.289	4.61	150.40
1.1	0.024	29	0.67	2.5	0.049	0.527	0.302	0.286	4.61	152.14
1.1	0.020	27	0.62	2.0	0.072	0.562	0.319	0.303	4.67	146.46
1.1	0.020	27	0.72	2.0	0.071	0.561	0.318	0.303	4.66	145.78
1.2	0.028	31	0.62	2.0	0.042	0.491	0.284	0.271	4.09	119.71
1.2	0.028	31	0.72	2.0	0.042	0.490	0.283	0.271	4.08	118.78
1.2	0.024	29	0.67	1.5	0.072	0.537	0.305	0.292	4.13	111.06
1.2	0.024	29	0.67	1.6	0.060	0.525	0.300	0.287	4.13	113.56
1.2	0.024	29	0.67	1.7	0.049	0.513	0.294	0.282	4.12	115.93
1.2	0.024	29	0.67	1.8	0.040	0.503	0.289	0.278	4.12	118.18
1.2	0.024	29	0.67	1.9	0.033	0.493	0.285	0.274	4.12	120.32
1.2	0.024	29	0.67	2.0	0.026	0.484	0.281	0.270	4.12	122.35
1.2	0.024	29	0.67	2.1	0.021	0.476	0.277	0.267	4.12	124.27
1.2	0.024	29	0.67	2.2	0.017	0.469	0.273	0.263	4.12	126.10
1.2	0.024	29	0.67	2.3	0.013	0.462	0.270	0.260	4.11	127.85
1.2	0.024	29	0.67	2.4	0.010	0.455	0.266	0.257	4.11	129.50
1.2	0.024	29	0.67	2.5	0.008	0.449	0.263	0.254	4.11	131.09
1.2	0.020	27	0.62	2.0	0.008	0.480	0.279	0.270	4.17	126.39
1.2	0.020	27	0.72	2.0	0.008	0.478	0.278	0.270	4.16	125.50

Mass [ $M_{\odot}$ ]	Z	Y	age [Gyr]	$\alpha$	U-B [mag]	B-V [mag]	V-R [mag]	R-I [mag]	$M_v$ [mag]	$\bar{\nu}_0$ [ $\mu\text{Hz}$ ]
1.3	0.028	31	0.62	2.0	0.025	0.428	0.251	0.243	3.65	103.66
1.3	0.028	31	0.72	2.0	0.025	0.428	0.251	0.243	3.64	102.54
1.3	0.024	29	0.67	1.5	0.024	0.460	0.268	0.261	3.68	97.16
1.3	0.024	29	0.67	1.6	0.020	0.451	0.264	0.256	3.68	99.07
1.3	0.024	29	0.67	1.7	0.017	0.443	0.259	0.253	3.68	100.92
1.3	0.024	29	0.67	1.8	0.014	0.435	0.255	0.249	3.68	102.68
1.3	0.024	29	0.67	1.9	0.013	0.428	0.252	0.245	3.68	104.36
1.3	0.024	29	0.67	2.0	0.012	0.422	0.248	0.242	3.68	105.97
1.3	0.024	29	0.67	2.1	0.011	0.416	0.245	0.239	3.68	107.50
1.3	0.024	29	0.67	2.2	0.011	0.410	0.242	0.236	3.67	108.97
1.3	0.024	29	0.67	2.3	0.011	0.404	0.238	0.233	3.67	110.39
1.3	0.024	29	0.67	2.4	0.011	0.399	0.236	0.230	3.67	111.74
1.3	0.024	29	0.67	2.5	0.011	0.395	0.233	0.227	3.67	113.05
1.3	0.020	27	0.62	2.0	-0.004	0.417	0.246	0.242	3.72	109.23
1.3	0.020	27	0.72	2.0	-0.004	0.416	0.246	0.241	3.70	108.17
1.4	0.028	31	0.62	2.0	0.033	0.380	0.224	0.219	3.26	90.35
1.4	0.028	31	0.72	2.0	0.034	0.382	0.225	0.220	3.25	89.01
1.4	0.024	29	0.67	1.5	0.020	0.399	0.235	0.232	3.29	85.61
1.4	0.024	29	0.67	1.6	0.020	0.394	0.232	0.229	3.29	87.03
1.4	0.024	29	0.67	1.7	0.021	0.389	0.229	0.226	3.28	88.41
1.4	0.024	29	0.67	1.8	0.021	0.384	0.226	0.223	3.28	89.75
1.4	0.024	29	0.67	1.9	0.022	0.378	0.223	0.220	3.28	91.04
1.4	0.024	29	0.67	2.0	0.023	0.374	0.221	0.217	3.28	92.29
1.4	0.024	29	0.67	2.1	0.023	0.369	0.218	0.214	3.28	93.49
1.4	0.024	29	0.67	2.2	0.024	0.364	0.215	0.212	3.28	94.65
1.4	0.024	29	0.67	2.3	0.025	0.360	0.213	0.209	3.28	95.78
1.4	0.024	29	0.67	2.4	0.026	0.356	0.210	0.207	3.28	96.88
1.4	0.024	29	0.67	2.5	0.026	0.352	0.208	0.204	3.28	97.94
1.4	0.020	27	0.62	2.0	0.009	0.366	0.217	0.215	3.32	95.31
1.4	0.020	27	0.72	2.0	0.010	0.367	0.218	0.216	3.30	94.05

Mass [ $M_{\odot}$ ]	Z	Y	age [Gyr]	$\alpha$	U-B [mag]	B-V [mag]	V-R [mag]	R-I [mag]	$M_v$ [mag]	$\nu_0$ [ $\mu\text{Hz}$ ]
1.5	0.028	31	0.62	2.0	0.050	0.340	0.200	0.197	2.91	79.25
1.5	0.028	31	0.72	2.0	0.050	0.344	0.202	0.200	2.90	77.59
1.5	0.024	29	0.67	1.5	0.038	0.344	0.203	0.201	2.93	78.03
1.5	0.024	29	0.67	1.6	0.038	0.342	0.202	0.200	2.93	78.44
1.5	0.024	29	0.67	1.7	0.039	0.340	0.201	0.199	2.93	78.90
1.5	0.024	29	0.67	1.8	0.040	0.338	0.199	0.198	2.93	79.53
1.5	0.024	29	0.67	1.9	0.040	0.335	0.197	0.196	2.93	80.28
1.5	0.024	29	0.67	2.0	0.041	0.331	0.196	0.194	2.93	81.10
1.5	0.024	29	0.67	2.1	0.042	0.328	0.194	0.192	2.93	81.99
1.5	0.024	29	0.67	2.2	0.043	0.325	0.192	0.190	2.93	82.89
1.5	0.024	29	0.67	2.3	0.045	0.322	0.190	0.188	2.93	83.80
1.5	0.024	29	0.67	2.4	0.046	0.319	0.188	0.186	2.93	84.67
1.5	0.024	29	0.67	2.5	0.048	0.315	0.186	0.184	2.93	85.51
1.5	0.020	27	0.62	2.0	0.031	0.321	0.190	0.190	2.97	84.23
1.5	0.020	27	0.72	2.0	0.030	0.324	0.192	0.192	2.95	82.64

Table 2: Model characteristics for stars evolved using M67 parameters.

Mass [ $M_{\odot}$ ]	Z	Y	$\alpha$	age [Gyr]	U-B [mag]	B-V [mag]	V-R [mag]	R-I [mag]	$M_{\nu}$ [mag]	$\bar{\nu}_0$ [ $\mu\text{Hz}$ ]
0.7	0.013	0.26	2.0	3.5	0.931	1.062	0.632	0.542	7.24	217.00
0.7	0.013	0.26	2.0	4.5	0.921	1.056	0.628	0.538	7.21	215.00
0.7	0.017	0.28	1.5	4.0	1.017	1.104	0.661	0.563	7.31	209.10
0.7	0.017	0.28	1.6	4.0	1.007	1.097	0.656	0.558	7.29	210.70
0.7	0.017	0.28	1.7	4.0	0.997	1.092	0.652	0.554	7.28	212.10
0.7	0.017	0.28	1.8	4.0	0.989	1.087	0.648	0.551	7.27	213.40
0.7	0.017	0.28	1.9	4.0	0.981	1.083	0.644	0.547	7.25	214.50
0.7	0.017	0.28	2.0	4.0	0.974	1.079	0.641	0.545	7.24	215.50
0.7	0.017	0.28	2.1	4.0	0.967	1.075	0.638	0.542	7.23	216.40
0.7	0.017	0.28	2.2	4.0	0.961	1.072	0.635	0.540	7.23	217.30
0.7	0.017	0.28	2.3	4.0	0.955	1.069	0.632	0.538	7.22	218.10
0.7	0.017	0.28	2.4	4.0	0.950	1.066	0.630	0.536	7.21	218.80
0.7	0.017	0.28	2.5	4.0	0.945	1.064	0.628	0.534	7.21	219.50
0.7	0.021	0.30	2.0	3.5	1.013	1.095	0.650	0.549	7.26	214.80
0.7	0.021	0.30	2.0	4.5	1.003	1.090	0.646	0.546	7.23	213.20
0.8	0.013	0.26	2.0	3.5	0.515	0.870	0.488	0.434	6.26	195.00
0.8	0.013	0.26	2.0	4.5	0.496	0.860	0.482	0.430	6.21	192.00
0.8	0.017	0.28	1.5	4.0	0.644	0.928	0.524	0.457	6.33	182.60
0.8	0.017	0.28	1.6	4.0	0.625	0.919	0.518	0.452	6.31	184.90
0.8	0.017	0.28	1.7	4.0	0.607	0.910	0.511	0.447	6.29	187.10
0.8	0.017	0.28	1.8	4.0	0.591	0.902	0.506	0.443	6.28	189.00
0.8	0.017	0.28	1.9	4.0	0.576	0.894	0.501	0.439	6.27	190.80
0.8	0.017	0.28	2.0	4.0	0.562	0.888	0.496	0.436	6.26	192.40
0.8	0.017	0.28	2.1	4.0	0.549	0.881	0.492	0.433	6.25	193.90
0.8	0.017	0.28	2.2	4.0	0.538	0.876	0.488	0.431	6.24	195.20
0.8	0.017	0.28	2.3	4.0	0.527	0.870	0.485	0.428	6.23	196.50
0.8	0.017	0.28	2.4	4.0	0.517	0.865	0.482	0.426	6.22	197.60
0.8	0.017	0.28	2.5	4.0	0.507	0.861	0.479	0.424	6.21	198.80
0.8	0.021	0.30	2.0	3.5	0.613	0.910	0.508	0.441	6.28	191.30
0.8	0.021	0.30	2.0	4.5	0.594	0.900	0.502	0.437	6.23	189.00

Mass [ $M_{\odot}$ ]	Z	Y	$\alpha$	age [Gyr]	U-B [mag]	B-V [mag]	V-R [mag]	R-I [mag]	$M_v$ [mag]	$\nu_0$ [ $\mu\text{Hz}$ ]
0.9	0.013	0.26	2.0	3.5	0.201	0.695	0.385	0.361	5.46	172.00
0.9	0.013	0.26	2.0	4.5	0.183	0.682	0.378	0.357	5.39	168.00
0.9	0.017	0.28	1.5	4.0	0.338	0.768	0.423	0.387	5.49	155.80
0.9	0.017	0.28	1.6	4.0	0.315	0.754	0.415	0.381	5.48	158.80
0.9	0.017	0.28	1.7	4.0	0.295	0.742	0.408	0.376	5.47	161.50
0.9	0.017	0.28	1.8	4.0	0.277	0.731	0.402	0.371	5.46	163.90
0.9	0.017	0.28	1.9	4.0	0.260	0.720	0.397	0.367	5.45	166.20
0.9	0.017	0.28	2.0	4.0	0.245	0.711	0.392	0.363	5.44	168.40
0.9	0.017	0.28	2.1	4.0	0.231	0.702	0.387	0.359	5.43	170.30
0.9	0.017	0.28	2.2	4.0	0.217	0.693	0.383	0.356	5.42	172.20
0.9	0.017	0.28	2.3	4.0	0.205	0.686	0.379	0.353	5.41	173.90
0.9	0.017	0.28	2.4	4.0	0.194	0.679	0.376	0.350	5.41	175.50
0.9	0.017	0.28	2.5	4.0	0.184	0.672	0.372	0.348	5.40	177.00
0.9	0.021	0.30	2.0	3.5	0.294	0.733	0.402	0.368	5.47	167.50
0.9	0.021	0.30	2.0	4.5	0.275	0.721	0.396	0.363	5.39	163.30
1.0	0.013	0.26	2.0	3.5	0.036	0.558	0.318	0.309	4.77	146.00
1.0	0.013	0.26	2.0	4.5	0.028	0.548	0.312	0.305	4.67	139.00
1.0	0.017	0.28	1.5	4.0	0.146	0.636	0.353	0.336	4.76	127.20
1.0	0.017	0.28	1.6	4.0	0.126	0.620	0.346	0.330	4.75	130.20
1.0	0.017	0.28	1.7	4.0	0.109	0.607	0.340	0.324	4.74	132.90
1.0	0.017	0.28	1.8	4.0	0.095	0.594	0.334	0.319	4.73	135.40
1.0	0.017	0.28	1.9	4.0	0.083	0.583	0.329	0.315	4.73	137.80
1.0	0.017	0.28	2.0	4.0	0.072	0.573	0.324	0.310	4.72	140.10
1.0	0.017	0.28	2.1	4.0	0.062	0.563	0.319	0.306	4.72	142.10
1.0	0.017	0.28	2.2	4.0	0.053	0.554	0.315	0.303	4.71	144.10
1.0	0.017	0.28	2.3	4.0	0.045	0.546	0.311	0.299	4.71	145.90
1.0	0.017	0.28	2.4	4.0	0.037	0.539	0.308	0.296	4.70	147.60
1.0	0.017	0.28	2.5	4.0	0.029	0.531	0.304	0.293	4.70	149.20
1.0	0.021	0.30	2.0	3.5	0.110	0.594	0.334	0.315	4.76	140.20
1.0	0.021	0.30	2.0	4.5	0.101	0.584	0.328	0.312	4.66	133.10

Mass [ $M_{\odot}$ ]	Z	Y	$\alpha$	age [Gyr]	U-B [mag]	B-V [mag]	V-R [mag]	R-I [mag]	$M_v$ [mag]	$\bar{\nu}_0$ [ $\mu\text{Hz}$ ]
1.1	0.013	0.26	2.0	3.5	-0.025	0.469	0.275	0.272	4.14	116.00
1.1	0.013	0.26	2.0	4.5	-0.020	0.469	0.274	0.273	4.01	106.00
1.1	0.017	0.28	1.5	4.0	0.061	0.546	0.309	0.302	4.09	99.40
1.1	0.017	0.28	1.6	4.0	0.049	0.533	0.303	0.296	4.09	101.70
1.1	0.017	0.28	1.7	4.0	0.037	0.521	0.298	0.291	4.09	104.00
1.1	0.017	0.28	1.8	4.0	0.027	0.510	0.293	0.286	4.08	106.10
1.1	0.017	0.28	1.9	4.0	0.018	0.500	0.288	0.282	4.08	108.10
1.1	0.017	0.28	2.0	4.0	0.011	0.490	0.284	0.278	4.08	109.90
1.1	0.017	0.28	2.1	4.0	0.004	0.481	0.280	0.274	4.08	111.70
1.1	0.017	0.28	2.2	4.0	-0.001	0.473	0.276	0.271	4.07	113.40
1.1	0.017	0.28	2.3	4.0	-0.006	0.466	0.272	0.267	4.07	114.90
1.1	0.017	0.28	2.4	4.0	-0.009	0.459	0.269	0.264	4.07	116.40
1.1	0.017	0.28	2.5	4.0	-0.012	0.452	0.266	0.261	4.07	117.80
1.1	0.021	0.30	2.0	3.5	0.038	0.508	0.292	0.282	4.14	112.10
1.1	0.021	0.30	2.0	4.5	0.054	0.522	0.298	0.288	4.04	102.10

## References

- Anders, E., & Grevesse, N. 1989, *Geochemica et Cosmochimica Acta*, 53, 197.
- Appourchaux, T., Catala, C., Catalano, S., Frandsen, S., Jones, A., Lemaire, P., Pace, O., Volonte, W., & Weiss, W. 1991, Report on the Assessment Study, Probing Rotation and Interior of Stars: Microvariability and Activity, ESA, SCI(91) 5.
- Biermann, L. 1932, *Z. Astrophys.*, 5, 117.
- Biermann, L. 1935, *A. N.*, 257, 269.
- Biermann, L. 1943, *Z. Astrophys.*, 22, 244.
- Biermann, L. 1948, *Z. Astrophys.*, 25, 135.
- Boesgaard, A. M. 1989, *Ap. J.*, 336, 798.
- Böhm-Vitense, E. 1958, *Z. Astrophys.*, 46, 108.
- Brown, T. M. 1991, in *Frontiers of Stellar Evolution*, ed. David L. Lambert (Astronomical Society of the Pacific, California), p. 139.
- Clayton, D. C. 1983, *Principles of Stellar Evolution and Nucleosynthesis* (McGraw-Hill, New York).
- Chaboyer, B., Demarque, P., & Pinsonneault, M. 1995, *Ap. J.*, 441, 876.
- Chaboyer, B., Demarque, P., Guenther, D., Pinsonneault, M., & Pinsonneault, L. 1995, in *The Formation of the Milky Way*, ed. E. J. Alfaro and G. Tenorio-Tagle (Cambridge University Press, Cambridge)
- Chen, K., & Sofia, S. 1987, *Science*, 235, 465.
- Cowling, T. J. 1935, *M. N. R. A. S.*, 96, 42.
- Cowling, T. J. 1936, *A. N.*, 258, 133.
- Cox, J. P., & Guili, R. T. 1968, *Principles of Stellar Structure* (Gordon and Breach, New York), Volume 1, p. 281.
- Demarque, P., Green, E., & Guenther, D. 1992, *A. J.*, 103, 151.

- Demarque, P., Krauss, L., Guenther, D., & Nydam, D. 1994, *Ap. J.*, 437, 870.
- Demarque, P. 1996, private communication.
- Deubner, F. 1975, *Astron. Astrophys.*, 44, 371.
- Dinescu, D., Demarque, P., Guenther, D., & Pinsonneault, M. 1995, *A. J.*, 109, 2090.
- Dombrowski, E., McAlister, H., Hartkopf, W., & Bagnuolo, W. 1991, *B. A. A. S.*, 23, 1329.
- Eddington, A. S. 1926, *The Internal Constitution of the Stars* (Cambridge University Press, Cambridge).
- Edmonds, P., Cram, L., Demarque, P., Guenther, D., & Pinsonneault, M. 1992, *Ap. J.*, 394, 313.
- Emden, R. 1907, *Gaskugeln*(Teubner, Berlin).
- Frazier, E. 1968, *Z. Astrophys.*, 68, 345.
- Gatewood, G., Castelaz, M., DeJonge, J., Persinger, T., Stein, J., & Stephenson, B. 1992, *Ap. J.*, 392, 710.
- Gelly, B., Grec, G., & Fossat, E. 1988, in *Advances in Helio- and Asteroseismology*, ed. J. Christensen-Dalsgaard and S. Frandsen (D. Reidel Publishing, Boston), p. 249.
- Gilliland, R., & Brown, T. 1992, *P. A. S. P.*, 104, 582.
- Gilliland, R., Brown, T., Kjeldsen, H., McCarthy, J., Peri, M., Belmonte, J., Vidal, I., Cram, L., Palmer, J., & Frandsen, S. 1993, *A. J.*, 106, 2441.
- Gough, D. 1987, *Nature*, 326, 257.
- Green, E., Demarque, P., & King, C. 1987, *Revised Yale Isochrones and Luminosity Functions* (Yale University Observatory, New Haven)
- Guenther, D. 1994, *Ap. J.*, 442, 400.
- Guenther, D., & Demarque, P. 1995, *Ap. J.*, 456, 798.
- Guenther, D., Jaffe, A., & Demarque, P. 1989, *Ap. J.*, 345, 1022.

- Guenther, D., Kim, Y-. C., Demarque, P. 1996, Ap. J., 463, 382.
- Iglesias, C., & Rogers, F. 1991, Ap. J., 371, 408.
- Kim, Y-. C., Guenther, D. B., & Demarque, P. 1996, Ap. J., in press.
- Kjeldsen, H., & Bedding, T. 1995, Astron. Astrophys., 293, 87.
- Kjeldsen, H., Bedding, T., Viskum, M., & Frandsen, S. 1995, A.J., 109, 1313.
- Kurucz, R. 1991, in *Stellar Atmospheres: Beyond Classical Models*, edited by L. Crivellani, I. Hubeny, & D. G. Hummer (Kluwer, Dordrecht), p. 440.
- Larson, R. B. 1974, *Fund. Cosmic Phys.*, 1, 1.
- Leighton, R., Noyes, R., & Simon, G. 1962, Ap. J., 135, 474.
- Montgomery, K., Marschall, L., & Janes, K. 1993, A. J., 106, 181.
- Nissen, P., Twarog, B., & Crawford, D. 1987, A. J., 93, 634.
- Peterson, D., Stefanik, R., & Latham, D. 1993, A. J., 105, 2260.
- Prandtl, L. 1925, *Z. Angew. Math. Mech.*, 5, 136.
- Schwarzschild, K. 1906, *Nachr. Kon. Gesselsch. d. Wiss., Gottingen*, No. 1.
- Schwarzschild, M. 1961, Ap. J., 134, 1.
- Tassoul, M. 1980, Ap. J. Suppl., 43, 469.
- Taylor, B. 1994, P. A. S. P., 106, 600.
- Tripicco, M., Dorman, B., & Bell, R. 1993, A. J., 106, 618.
- Ulrich, R. 1970, Ap. J., 162, 993.
- Vandakurov, Yu. 1967, *Astron. Zh.* 44, 786.
- VandenBerg, D., & Poll, H. 1989, A. J., 98, 1451.
- Vitense, E. 1953, *Z. Astrophys.*, 32, 135.

## Curriculum Vitae

- Name:* Kenneth Royal Sills
- Date and place of birth:* 21 December 1970, Windsor, Ontario, Canada
- Post-secondary education:* University of Western Ontario, London, Ontario, Canada  
1989-1993 Bachelor of Science  
Saint Mary's University, Halifax, Nova Scotia, Canada  
1994-1996 Master of Science
- Current Employment:* Research Assistant, Advanced Fuel Research,  
East Hartford, Connecticut, USA
- Honours and Awards:* Father Burke-Gaffney Memorial Scholarship,  
Saint Mary's University, 1994  
Saint Mary's University Graduate Award, 1993  
NSERC summer student fellowship, 1990
- Related Work Experience:* Teaching and Research Assistant,  
Saint Mary's University, 1994-1995  
Teaching Assistant,  
University of Western Ontario, 1991-1993

### *Publications:*

1. Mitalas, R. and **Sills, K. R.** On the photon diffusion time scale for the sun ApJ, 401 759, 1992
2. Guenther, D. B., **Sills, K.**, Demarque, P., Krauss, L. M. Sensitivity of solar g-modes to varying G cosmologies ApJ 445, 148, 1995